

# Microfabricated Monolithic Multinozzle Emitters for Nanoelectrospray Mass Spectrometry

Woong Kim,<sup>†</sup> Mingquan Guo,<sup>‡</sup> Peidong Yang,<sup>\*,†,§</sup> and Daojing Wang<sup>\*,†</sup>

The Molecular Foundry, Materials Sciences Division, and Life Sciences Division, Lawrence Berkeley National Laboratory, Berkeley, California 94720, and Department of Chemistry, University of California, Berkeley, California 94720

Mass spectrometry is the enabling technology for proteomics. To fully realize the enormous potential of lab-on-a-chip in proteomics, a major advance in interfacing microfluidics with mass spectrometry is needed. Here, we report the first demonstration of monolithic integration of multinozzle electrospray emitters with a microfluidic channel via a novel silicon microfabrication process. These microfabricated monolithic multinozzle emitters ( $M^3$  emitters) can be readily mass-produced from silicon wafers. Each emitter consists of a parallel silica nozzle array protruding out from a hollow silicon sliver with a conduit size of  $100 \times 10 \mu\text{m}$ . The dimension and number of freestanding nozzles can be systematically and precisely controlled during the fabrication process. Once integrated with a mass spectrometer,  $M^3$  emitters achieved sensitivity and stability in peptide and protein detection comparable to those of commercial silica-based capillary nanoelectrospray tips. These  $M^3$  emitters may play a role as a critical component in a fully integrated silicon/silica-based micro total analysis system for proteomics.

Mass spectrometry (MS) remains the central tool for proteomics.<sup>1,2</sup> Technological developments in MS have been a multifaceted and open-ended endeavor. Two current focuses are as follows: (1) continuing improvement in detection sensitivity, resolution, and mass accuracy; and (2) miniaturization of both front-end sample preparation and back-end mass detection. For example, a hybrid linear ion trap/orbitrap mass spectrometer has recently been shown to provide a mass accuracy of up to 2 ppm and a resolving power exceeding 100 000 (fwhm).<sup>3</sup> Microfluidic liquid chromatography–mass spectrometry platforms based on polymer parylene<sup>4</sup> or polyimide films<sup>5</sup> have been demonstrated. A handheld

rectilinear ion trap mass spectrometer has recently been built.<sup>6</sup> However, proteome-on-a-chip still remains a challenge due to the lack of technology for a high-quality interface between microfluidic channels and mass spectrometers.<sup>7</sup>

Despite recent development of new ionization sources such as desorption electrospray ionization,<sup>8</sup> matrix-assisted laser desorption/ionization and electrospray ionization (ESI) remain the dominant soft ionization methods for peptides and proteins. Since Fenn et al. first demonstrated the utility of ESI mass spectrometry in analyzing high molecular weight biomolecules,<sup>9</sup> extensive scientific and engineering efforts have been made to understand the mechanism of electrospray ionization process and to improve the performance of ESI-MS. One of the most significant steps along this line is the theoretical description and experimental demonstration of nanoelectrospray ionization (nanoESI)<sup>10</sup> and its applications in protein analysis.<sup>11</sup> However, the fundamental difference between conventional ESI and nanoESI has not yet been fully elucidated.<sup>12</sup>

Microfabricated monolithic nanoESI emitters have the potential to contribute to both technological developments and theoretical understanding of nanoelectrospray mass spectrometry. First, they can be mass-produced by microfabrication technology and readily interfaced with microfluidic channels in a lab-on-a-chip proteomic system. Second, they provide a means to systematically alter the size, shape, and density of electrospray nozzles so that fundamental mechanisms underlying the electrospray ionization process can be studied. There have been efforts to fabricate ESI emitters using either polymeric materials or silicon-based materials. The former includes nozzles made of parylene,<sup>13,14</sup> poly(dimethylsiloxane),<sup>15</sup> poly(methyl methacrylate),<sup>16</sup> and a negative photoresist

\* To whom correspondence should be addressed. E-mail: djwang@lbl.gov; p\_yang@uclink.berkeley.edu.

<sup>†</sup> The Molecular Foundry, Materials Sciences Division, Lawrence Berkeley National Laboratory.

<sup>‡</sup> Life Sciences Division, Lawrence Berkeley National Laboratory.

<sup>§</sup> University of California.

- (1) Aebersold, R.; Mann, M. *Nature* **2003**, *422*, 198–207.
- (2) Domon, B.; Aebersold, R. *Science* **2006**, *312*, 212–217.
- (3) Makarov, A.; Denisov, E.; Kholomeev, A.; Baischun, W.; Lange, O.; Strupat, K.; Horning, S. *Anal. Chem.* **2006**, *78*, 2113–2120.
- (4) Xie, J.; Miao, Y. N.; Shih, J.; Tai, Y. C.; Lee, T. D. *Anal. Chem.* **2005**, *77*, 6947–6953.
- (5) Yin, H.; Killeen, K.; Brennen, R.; Sobek, D.; Werlich, M.; van de Goor, T. V. *Anal. Chem.* **2005**, *77*, 527–533.

(6) Gao, L.; Song, Q. Y.; Patterson, G. E.; Cooks, R. G.; Ouyang, Z. *Anal. Chem.* **2006**, *78*, 5994–6002.

(7) Freire, S. L. S.; Wheeler, A. R. *Lab Chip* **2006**, *6*, 1415–1423.

(8) Takats, Z.; Wiseman, J. M.; Gologan, B.; Cooks, R. G. *Science* **2004**, *306*, 471–473.

(9) Fenn, J. B.; Mann, M.; Meng, C. K.; Wong, S. F.; Whitehouse, C. M. *Science* **1989**, *246*, 64–71.

(10) Wilm, M. S.; Mann, M. *Int. J. Mass Spectrom. Ion Processes* **1994**, *136*, 167–180.

(11) Wilm, M.; Shevchenko, A.; Houthaeve, T.; Breit, S.; Schweigerer, L.; Fotsis, T.; Mann, M. *Nature* **1996**, *379*, 466–469.

(12) Juraschek, R.; Dulcks, T.; Karas, M. *J. Am. Soc. Mass Spectrom.* **1999**, *10*, 300–308.

(13) Licklider, L.; Wang, X. Q.; Desai, A.; Tai, Y. C.; Lee, T. D. *Anal. Chem.* **2000**, *72*, 367–375.

(14) Yang, Y. N.; Kameoka, J.; Wachs, T.; Henion, J. D.; Craighead, H. G. *Anal. Chem.* **2004**, *76*, 2568–2574.

(15) Kim, J. S.; Knapp, D. R. *J. Am. Soc. Mass Spectrom.* **2001**, *12*, 463–469.

SU-8.<sup>17,18</sup> The latter includes nozzles made of silicon nitride using in-plane fabrication<sup>19</sup> and of silicon/silica using out-of-plane processes.<sup>20,21</sup> However, hydrophobic polymers have inherently undesirable properties for the electro spray application, such as strong affinity to proteins and incompatibility with certain organic solvents.<sup>22,23</sup> In-plane fabrication was not pursued further apparently due to the intrinsic clogging problem arising from the etching of a sacrificial layer of phosphosilicate glass between two layers of silicon nitride.<sup>19</sup> Out-of-plane fabrication is critically limited in terms of the flexibility to produce monolithically integrated built-in structures and requires additional assembly steps to attach nozzles to the end of a microfluidic channel. More recent efforts to generate nanoelectrospray from a nanofluidic capillary slot<sup>24</sup> and a micromachined ultrasonic ejector array<sup>25</sup> faced similar challenges.

Here, we report a novel silicon/silica-based microfabrication process that is straightforward and flexible for the monolithic fabrication of biocompatible M<sup>3</sup> emitters. Our fabrication process requires only one mask and consists of five major steps (Figure 1). A photolithographic patterning step defines the size and the shape of the microfluidic channels (Figure 1a). Deep reactive ion etching combined with silicon fusion bonding encloses the microfluidic channels (Figure 1b,c). Oxidation and XeF<sub>2</sub> etching generate protruding nanoelectrospray nozzles made of SiO<sub>2</sub> (Figure 1d,e). The process is significantly simplified compared to the previous examples<sup>19–21</sup> and generates biocompatible, monolithic, microfluidic channels connected with multinozzles. A distinctive advantage of our process is its versatility and its amenability for large-scale production. The nanoelectrospray emitters with various size and number of protruding nozzles were monolithically fabricated with unprecedentedly high array density (line density = 100 nozzles/mm).

## EXPERIMENTAL SECTION

**Microfabrication of Nanoelectrospray Emitters.** A layout of microfluidic channels (~6 cm long) were photolithographically patterned on a (100) p-type silicon wafer of 4-in. diameter ( $\rho = 15\text{--}30 \Omega \text{ cm}$ ). After the development of the exposed photoresist, the area for the channels was etched down via a deep reactive ion etching process using the advanced silicon etching system from Surface Technology Systems. The depths of the channels were measured using a surface profiler. After the removal of the photoresist, the wafer was cleaned in piranha solution at 120 °C, thoroughly rinsed with deionized water (~18 M $\Omega$ ), and spun dry. Immediately after the cleaning and drying step, the patterned

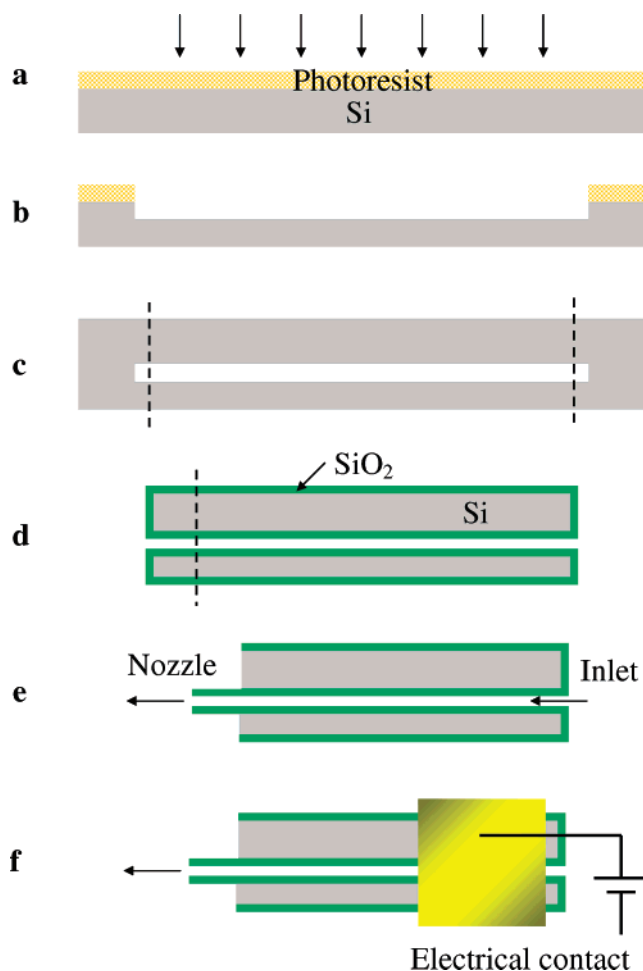


**Figure 1.** Microfabrication process of multinozzle nanoelectrospray emitters: (a) photolithographic patterning of microfluidic channels, (b) development of photoresist and deep reactive ion etching of the channels, (c) silicon fusion bonding with a plane wafer and opening the channels on both side of the wafer, (d) thermal oxidation and wafer cutting to expose silicon on nozzle side, (e) selective silicon etching against SiO<sub>2</sub> by XeF<sub>2</sub>, and (f) electrical contact to the conductive silicon on the side of a M<sup>3</sup> emitter.

wafer was gently pressed with a clean plane wafer under a sink equipped with high-efficiency particulate air filters. These prebonded wafer pairs were then annealed in the stream of N<sub>2</sub> flow at 1050 °C for 1 h for silicon–silicon fusion bonding, which generates covalent bonding between the two wafers.

After the aforementioned channel etching and the wafer bonding steps, the microfluidic channels were enclosed inside the bonded wafer. To open up each side of the channels, both sides of the wafer were cut using an automatic wafer saw. After that, SiO<sub>2</sub> was thermally grown on the wafer including the surface of the open channel inside the wafer. The wet oxidation process at 1050 °C for 10 h yielded the oxide with a thickness of ~1.9  $\mu\text{m}$ . Around 2–3 mm of nozzle side of the wafer was cut off to remove SiO<sub>2</sub> capping layer and expose silicon at this end of the wafer. After the wafer was cut into individual electro spray tips, the exposed silicon at the ends of the tips was selectively etched away against SiO<sub>2</sub> using XeF<sub>2</sub> as the etching gas. This selective silicon etching step leaves behind protruding nozzles made of SiO<sub>2</sub> (length ~200  $\mu\text{m}$ ). The tips went through 200–250 cycles of XeF<sub>2</sub> etching and N<sub>2</sub> purging. Each etching step was carried out for 60 s under the pressure of 4 Torr of XeF<sub>2</sub> and 2 Torr of N<sub>2</sub>.

- (16) Schilling, M.; Nigge, W.; Rudzinski, A.; Neyer, A.; Hergenroder, R. *Lab Chip* **2004**, *4*, 220–224.
- (17) Le Gac, S.; Arscott, S.; Rolando, C. *Electrophoresis* **2003**, *24*, 3640–3647.
- (18) Nordstrom, M.; Marie, R.; Calleja, M.; Boisen, A. *J. Micromech. Microeng.* **2004**, *14*, 1614–1617.
- (19) Desai, A.; Tai, Y.; Davis, M. T.; Lee, T. D. International Conference on Solid State Sensors and Actuators (Transducers '97), Piscataway, NJ, 1997; pp 927–930.
- (20) Schultz, G. A.; Corso, T. N.; Prosser, S. J.; Zhang, S. *Anal. Chem.* **2000**, *72*, 4058–4063.
- (21) Griss, P.; Melin, J.; Sjodahl, J.; Roeraade, J.; Stemme, G. *J. Micromech. Microeng.* **2002**, *12*, 682–687.
- (22) Huang, B.; Wu, H. K.; Kim, S.; Zare, R. N. *Lab Chip* **2005**, *5*, 1005–1007.
- (23) Lee, J. N.; Park, C.; Whitesides, G. M. *Anal. Chem.* **2003**, *75*, 6544–6554.
- (24) Arscott, S.; Troadec, D. *Appl. Phys. Lett.* **2005**, *87*, 134101.
- (25) Aderogba, S.; Meacham, J. M.; Degertekin, F. L.; Fedorov, A. G.; Fernandez, F. M. *Appl. Phys. Lett.* **2005**, *86*, 203110.

**Nanoelectrospray Mass Spectrometry.** All electro-spray ionization mass spectrometry experiments were performed on a hybrid quadrupole/orthogonal time-of-flight mass spectrometer Q-TOF API US (Waters, MA). The mass spectrometer was operated in a positive ion mode with a source temperature of 120 °C and a cone voltage of 40 V. A voltage of 2 kV was applied to the PicoTip emitter (New Objectives). TOF analyzer was set in the V-mode. The instrument was calibrated with a multipoint calibration using selected fragment ions from the collision-induced decomposition of Glu-fibrinopeptide B (GFP B). Except the electro-spray voltages applied, identical instrument conditions were utilized for fabricated  $M^3$  emitters and commercial tips during the comparison. Electrical contact was made via an aluminum tape to the side of the  $M^3$  emitters, where conductive silicon was exposed after being cut into individual emitters (Figure 1f).

GFP B was purchased from Sigma and dissolved in a solvent of 30% acetonitrile and 0.1% formic acid in deionized water. Bovine serum albumin and myoglobin were purchased from Amersham Biosciences and Sigma, respectively, and prepared in the same way as the GFP B solution. All analyte solutions were at 1  $\mu$ M concentration. The analyte solutions were directed to the electro-spray emitters through a 500- $\mu$ L syringe. A syringe pump was used to maintain a constant flow rate. A capillary tube (i.d.  $\sim$ 75  $\mu$ m) from the syringe was connected to the fabricated electro-spray emitters via Teflon tubes. Epoxy adhesive was applied to seal the connection and was cured overnight at room temperature before use.

## RESULTS AND DISCUSSION

**Microfabrication and Examination of  $M^3$  Emitters.** We have incorporated microelectromechanical system techniques in the fabrication process. For example, the channels were etched and enclosed between two wafers by the combination of deep reactive ion etching and silicon fusion bonding techniques. This combination is a versatile tool and has been demonstrated to fabricate various micromechanical devices.<sup>26</sup> In the etching step, silicon channels are etched down via time-multiplexed  $SF_6$  etching and  $C_4F_8$  passivation cycles.<sup>27</sup> In the bonding step, two piranha-cleaned wafers are first held together via hydrogen bonding between the silanol groups of the surfaces of each wafer. Subsequent high-temperature annealing of the prebonded wafers enables the formation of the Si–O–Si covalent bonds at the interface of the wafers. The bond strength of these wafers is on the order of the yield strength of single-crystal silicon ( $\sim$ 1 GPa).<sup>28</sup> This feature makes our microfluidic structures practically monolithic and imparts high bonding quality against leakage and rupture. No physical gap at the interface was observed under scanning electron microscopy (SEM), and no fluid leakage was detected during the operation of electro-spray mass spectrometry. Since hydrophilicity of the channel was very important for the capillary action to occur, all channels were treated with piranha solution before use. Owing to the hydrophilic properties of  $SiO_2$ , our electro-spray emitters are intrinsically more compatible with

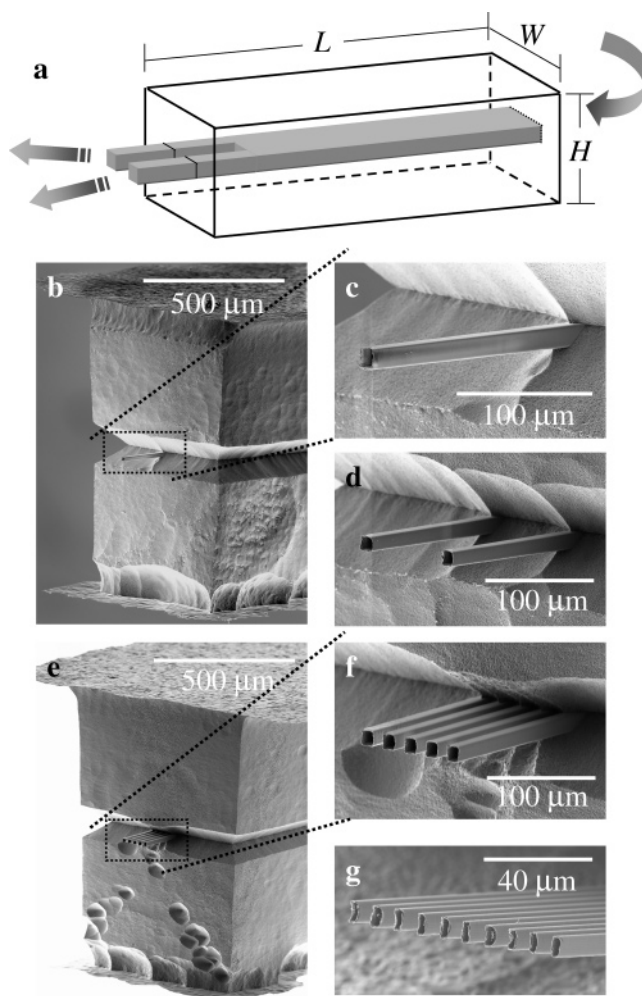


**Figure 2.** (a) Schematic view of a nanoelectrospray emitter with two protruding nozzles.  $L = 5.5$  cm,  $W = 0.6$  mm,  $H = 1$  mm. The length of the protruding part of the nozzles is  $\sim$ 200  $\mu$ m (not to scale). (b) SEM image of a protruding single-nozzle spray emitter. (c) Magnified image of the nozzle that is 10  $\mu$ m wide and 12  $\mu$ m deep. (d) Double-nozzle emitter (10  $\times$  12  $\mu$ m). (e) Five-nozzle emitter. (f) Zoom-in image of (e) (10  $\times$  12  $\mu$ m nozzle). (g) Ten-nozzle emitter (2  $\mu$ m wide and 8  $\mu$ m deep nozzle).

various biomolecules than hydrophobic polymer-based electro-spray emitters.

SEM was used to examine the microfabricated structures (Figure 2b–g). A schematic view of the  $M^3$  emitters is shown in Figure 2a. The final product is a silicon sliver that consists of an embedded microfluidic channel that is 100  $\mu$ m wide and 10  $\mu$ m deep and monolithically integrated silica multinozzles. The nozzles protrude about 150–250  $\mu$ m from the end of silicon stem. These protruding nozzles are made of  $SiO_2$  and are the result of the selective etching of surrounding Si by  $XeF_2$ . The selectivity of Si etching against  $SiO_2$  was roughly 400 to 1. The oxide thickness of the nozzle tips was  $\sim$ 1  $\mu$ m after the etching step. It was reported that the elastic modulus of a  $SiO_2$  beam with similar thickness was  $\sim$ 85 GPa, as measured by atomic force microscopy.<sup>29</sup>

Our process is straightforward but not limited in fabricating complicated structures. For example, multiple nozzles were

(26) Klaassen, E. H.; Petersen, K.; Noworolski, J. M.; Logan, J.; Maluf, N. I.; Brown, J.; Storment, C.; McCulley, W.; Kovacs, G. T. A. *Sens. Actuators, A* **1996**, *52*, 132–139.

(27) Blaw, M. A.; Zijlstra, T.; van der Drift, E. *J. Vac. Sci. Technol., B* **2001**, *19*, 2930–2934.

(28) Barth, P. W. *Sens. Actuators, A* **1990**, *23*, 919–926.

(29) Sundararajan, S.; Bhushan, B.; Namazu, T.; Isono, Y. *Ultramicroscopy* **2002**, *91*, 111–118.

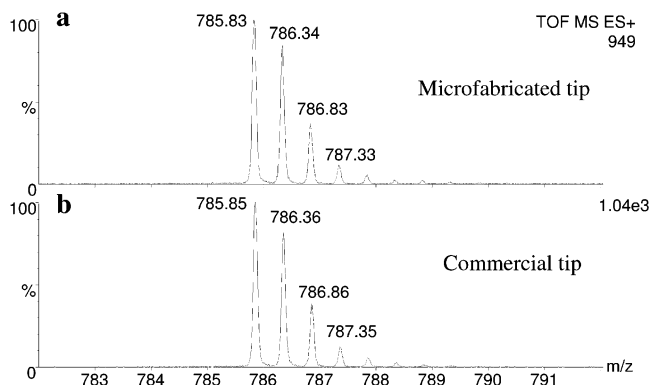


**Figure 3.** Mass spectra of 1  $\mu\text{M}$  GFP B obtained from (a) a single-nozzle emitter ( $10\ \mu\text{m} \times 8\ \mu\text{m}$ ) and (b) a commercial capillary tip (i.d.  $\sim 10\ \mu\text{m}$ ). Voltages of 4.5 and 2.1 kV were applied to the fabricated emitters and the commercial tips, respectively. The flow rate was 0.6  $\mu\text{L}/\text{min}$  for all tips.

fabricated at the end of electrospray emitters (Figure 2d–g). Panels e and f in Figure 2 show five  $10\ \mu\text{m} \times 12\ \mu\text{m}$  ( $W \times D$ ) nozzles branching out of the main channel, which has a cross-sectional area that is  $100\ \mu\text{m}$  wide and  $12\ \mu\text{m}$  deep. Internozzle space in this case is  $\sim 10\ \mu\text{m}$ . Figure 2g shows an array of 10 protruding nozzles ( $2\ \mu\text{m} \times 8\ \mu\text{m}$ ) in the cross-sectional area of  $100\ \mu\text{m} \times 8\ \mu\text{m}$  of a main channel. It approximately corresponds to a linear density of 100 nozzles/mm. This is an unprecedentedly high nozzle density. Extension of one-dimensional (1D) to two-dimensional (2D) arrays is possible by multistacking of 1D arrays using thinner wafers ( $\sim 100\ \mu\text{m}$ ), which should result in an areal density of  $10^3/\text{mm}^2$ . For comparison, a nozzle array with density of 2.5 nozzles/ $\text{mm}^2$  was recently fabricated via an out-of-plane approach.<sup>30</sup> Using the same process and by only changing the layout, complex built-in structures composed of a separation column,<sup>5</sup> a sample reservoir,<sup>7</sup> and a particle filter<sup>19</sup> can be monolithically fabricated at the main channel side as well. With further optimization and with the help of E-beam lithography or nanoimprint technology, it is also possible to fabricate  $\text{M}^3$  emitters down to submicrometers in nozzle size and up to  $10^5$  nozzles/ $\text{mm}^2$  in density. A total of 55 emitters with various numbers and sizes of nozzles were fabricated on a bonded wafer, and this number can be easily increased by several factors by optimizing the dimensions and layout of the emitters.

#### Nanoelectrospray Mass Spectrometry Using $\text{M}^3$ Emitters.

We first tested the viability of these novel  $\text{M}^3$  emitters using organic solvents. The solvents were delivered to the inlet of the sliver stem that had a rectangular opening of  $100\text{-}\mu\text{m}$  width and  $10\text{-}\mu\text{m}$  depth (Figure 2a). The solution then passed through the slablike hollow channel and sprayed off from the nozzles ( $10\ \mu\text{m} \times 10\ \mu\text{m}$ ) at the other side of the stem. The length, width, and height of the whole chip were approximately 5.5 cm, 600  $\mu\text{m}$ , and 1 mm, respectively. These dimensions were made similar to those of pulled-out capillary nanoelectrospray tips (purchased from New Objective, Inc.) used for comparison in this study (length  $\sim 7.5$  cm, outer diameter of the capillary  $\sim 360\ \mu\text{m}$ , and inner diameter of orifice  $\sim 10\ \mu\text{m}$ ). We observed that the protrusion of the nozzles was critical for generating electrospray ionization. It isolated initial

(30) Deng, W. W.; Klemic, J. F.; Li, X. H.; Reed, M. A.; Gomez, A. J. *Aerosol Sci.* **2006**, *37*, 696–714.

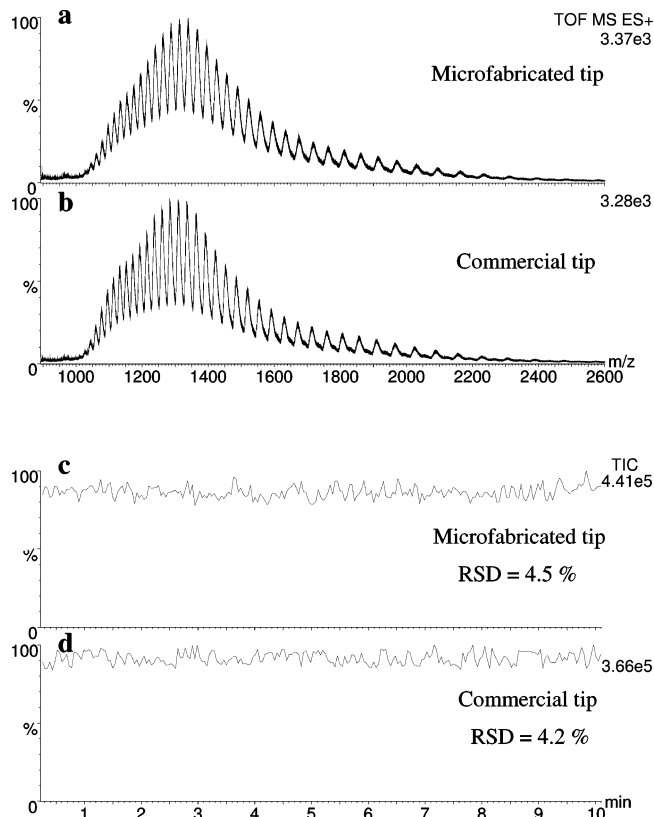


**Figure 4.** Mass spectra of 1  $\mu\text{M}$  BSA obtained from (a) a single-nozzle emitter and (b) a commercial tip. Total ion counts of 1  $\mu\text{M}$  BSA over time obtained from (c) the single-nozzle emitter and (d) the commercial tip. The RSD was 4.5 and 4.2%, respectively.

liquid droplets at the tips of nozzles from the surface of the silicon stem and prevented the droplets from wetting the surface. When the length of the nozzles was below tens of micrometers, no electrospray was observed due to the wetting problem, similar to the case of flat edge tips. The difficulty of the electrospray generation from flat edge tips due to the surface tension was reported previously.<sup>31</sup>

We then tested the performance of the  $\text{M}^3$  emitters for potential proteomic applications. We used  $\text{M}^3$  emitters containing a single nozzle ( $10\ \mu\text{m} \times 8\ \mu\text{m}$ ) and did a head-to-head comparison with commercially available, pulled fused-silica capillary nanoelectrospray tips with an orifice inner diameter of  $\sim 10\ \mu\text{m}$  (SilicaTips, New Objective, Inc.). The  $\text{M}^3$  emitters were integrated with a Q-TOF mass spectrometer (Waters Inc.). Since the emitters were made of conductive silicon, they were used without additional metal coatings. In contrast, most of the commercial silica-based ESI tips need to be coated with Pt or Au. First, a standard peptide, GFP B (MW = 1570.57) was tested. The GFP B solution (1  $\mu\text{M}$ ) was delivered to the nozzle at a flow rate of 600 nL/min, as described in the Experimental Section. Panels a and b in Figure 3 show the mass spectra obtained from the fabricated emitter and the commercial tip, respectively. The isotopic distributions of doubly charged ions of GFP B were clearly observed, and similar magnitudes of base peak intensity (BPI) of  $\sim 1000/\text{scan}$  were obtained in both cases. This indicates that the resolution and the

(31) Xue, Q. F.; Foret, F.; Dunayevskiy, Y. M.; Zavracky, P. M.; McGruer, N. E.; Karger, B. L. *Anal. Chem.* **1997**, *69*, 426–430.

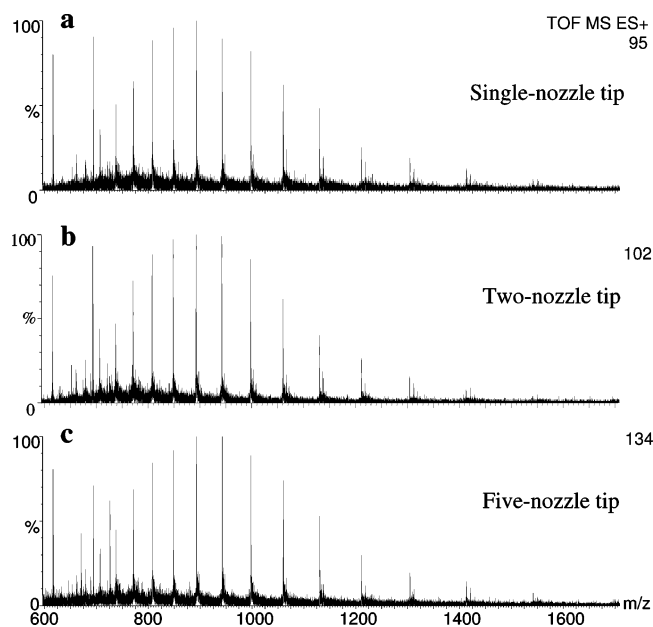


**Figure 5.** Mass spectra of 1  $\mu\text{M}$  myoglobin obtained from (a) a single-nozzle emitter, (b) a two-nozzle emitter, and (c) a five-nozzle emitter.

sensitivity of our fabricated emitters are comparable to those of commercial tips. However, higher voltage (4.5–4.8 kV) was needed for the fabricated emitters than for the commercial tips (2.1–2.4 kV). We conjecture that depositing metal on the tips or using more conductive silicon wafers may lower the required voltage. Since we were using a platform that was already optimized for the commercial tips, detailed optimization on any electrical and mechanical connections of the fabricated emitters may lower the voltage as well.

Since detecting masses of full-length proteins is equally important as detecting those of proteolytic peptides in proteomics, we further compared the performance of our  $M^3$  emitters with commercial tips for detecting high molecular weight proteins. Similar results were obtained as shown in the mass spectra of bovine serum albumin (BSA,  $\sim 67$  kDa) that were accumulated for 10 min (Figure 4a,b). Charge-state distribution and base peak intensity were similar in both cases. They showed 38 or more charge states of the protein with the highest peak at around 1340, which corresponds to  $\sim 50$  positive charges. Panels c and d in Figure 4 show that the stability of our emitters (relative standard deviation, RSD  $\sim 4.5\%$ ) is comparable to that of a commercial tip (RSD  $\sim 4.2\%$ ).

Finally, our unique microfabrication process enables direct performance comparison between a multinozzle emitter ( $10 \mu\text{m} \times 12 \mu\text{m}$ ) and a single-nozzle emitter ( $10 \mu\text{m} \times 12 \mu\text{m}$ ). Since the flow rate at the main channel was kept constant at 600 nL/min, the flow rate at each nozzle on average was 120 nL/min for the five-nozzle emitter. Mass spectra of myoglobin ( $\sim 17$  kDa) obtained from a single-, a dual-, and a five-nozzle emitter are shown in Figure 5. Electrospray was observed from each of the five nozzles. However, two outer nozzles generated bigger droplets similarly to those observed and described in a large-scale multinozzle spray previously.<sup>30</sup> In general, multinozzle emitters showed similar performance yet slightly higher sensitivity than that of the single-nozzle emitters. Multinozzle emitters are expected to ease back pressure and clogging problems that single-nozzle emitters have to cope with, especially as the channel downsizes to submicrometer scale. In addition, high-density multinozzle emitters provide a valuable means to study the ionization process since extremely low flow rate can be achieved at each single nozzle.

## CONCLUSIONS

We presented a novel and significantly simplified procedure for the microfabrication of fully integrated nanoelectrospray emitters. It consists of an etching and silicon fusion bonding step for the formation of enclosed channel and an oxidation and  $\text{XeF}_2$  etching step for the formation of protruding multinozzles. These microfabricated monolithic multinozzle emitters ( $M^3$  emitters) showed a performance comparable to that of the commercial tips in terms of stability and sensitivity for a standard peptide and high molecular weight proteins. With further device optimization, additional performance enhancement is expected. Our process is straightforward, yet fully capable of producing complicated structures such as a high-density array of overhanging nozzles that are monolithically integrated with a microfluidic channel. The simplicity and the versatility of our process may be potentially utilized to fabricate other complex bioanalytical tools.

## ACKNOWLEDGMENT

This work was supported by National Institutes of Health Grant R21GM077870 (to D.W.). Part of this work was performed at the Molecular Foundry, Lawrence Berkeley National Laboratory, which is supported by the Office of Science, Office of Basic Energy Sciences, of the U.S. Department of Energy under Contract DE-AC02-05CH11231.

Received for review January 2, 2007. Accepted March 19, 2007.

AC070010J